

## CHAPTER 4

### LOADING ATOMS INTO DIPOLE TRAP

After the preparation of cold Rb atoms was achieved at the QAO Laboratory, the generation of a single atom in an optical dipole trap and the two-body collisions of cold  $^{85}\text{Rb}$  atoms were studied by using an apparatus at the Otago Atomic Physics Laboratory at the University of Otago in New Zealand. In this chapter, the apparatus setup including the methodology for loading cold Rb atoms into an optical dipole trap are reported in Section 4.1 and the result of detection of the atoms in the trap is represented in Section 4.2.

#### 4.1 Apparatus for loading the dipole trap

The main parts of the apparatus for cooling and confining  $^{85}\text{Rb}$  atoms in the dipole trap or the far-off-resonance optical trap (FORT) are reported. This section begins with the details of the vacuum system in Section 4.1.1 and the cooling system in Section 4.1.2, which are similar to the system in QAO Laboratory. Using the vacuum and cooling systems loaded cold MOT atoms. Consequently, the atoms were transferred into the far-off-resonance dipole trap (FORT) via the compressed MOT (cMOT) and the following optical molasses. The atoms in FORT were observed by using an imaging stage. The details of the dipole trap and the imaging system are provided in Section 4.1.3 and Section 4.1.4 respectively.

### 4.1.1 Vacuum system

As described before in Chapter 3, it is necessary to prepare the cold  $^{85}\text{Rb}$  atoms in the vacuum system. This vacuum system is divided in two parts, an Rb-atom reservoir and an ultra-high vacuum (UHV) system. For the atom reservoir, a 1 g of natural Rb metal was put in a reservoir chamber, of which temperature were controlled by a thermoelectric device (see Figure 4.1). Adjusting the temperature could change the evaporation rate of the Rb atoms. To separate this chamber, a MDC gate valve (Part No.: GV-1500M) was mounted at the reservoir chamber as shown in the figure. The other end of the vale was connected to a six-way cross where the evaporated Rb atoms (from the reservoir chamber) were accumulated inside. One port of this cross was connected to an Agilent VacIon Plus 20 Diode Ion Pump for keeping high vacuum. The other ports were connected to the second thermoelectric device for controlling temperature, an MDC angle valve (Part No.: MAV-150V) for installing a turbo-molecular pump and the second gate vale for isolating this Rb source system from a science chamber. This Rb source system fed the atoms into the UHV part through a home-built differential pumping tube.

Figure 4.2 shows a schematic of the UHV system. Below the Rb source system, there was a science chamber where the cold atoms were loaded. The chamber was a Kimball  $2\frac{3}{4}$  multi-CF spherical cube (Part No.: MFC275-ESC608). It consisted of six ports of a  $2\frac{3}{4}$ -inch CF flange and eight ports of an  $1\frac{1}{3}$ -inch CF flange. One of the  $1\frac{1}{3}$ -inch port was connected to the differential pumping tube as mentioned before, another one was fitted with a high numerical aperture (NA) lens



used for the dipole trap formation, and the others were fitted with anti-reflection coated view ports. Five of the  $2\frac{3}{4}$ -inch ports were also fitted with the view ports. A six-way cross was mounted on the last  $2\frac{3}{4}$ -inch port for connecting the science chamber to a Vacuum Generators ST22 Titanium (Ti) Sublimation pump, an Agilent VacIon Plus 75 Starcell Ion pump, and a SenTorr Ion Gauge. One port of the six-way cross was fitted with the view port where a laser light was applied into the science chamber as shown in the figure. For keeping the pressure of the UHV system in the order of  $1 \times 10^{-11}$  Torr, the Ion pump was left on all the time and the Ti sublimation pump was weekly used by applying the current of 46 A for one minute.

#### 4.1.2 Cooling system

For loading atoms into the dipole trap, it is necessary to start with loading the MOT, of which the process was the same as detailed in Chapter 3. Two lasers were needed for generating the MOT/cooling beams and the MOT repump beam. A Toptica TA-100 ECDL with a tapered amplifier was used to provide the MOT/cooling beam. As shown in Figure 4.3, the laser beam with a measured power of about 356 mW at 780 nm wavelength was split a few mW into a DSAS part for locking the laser frequency at the crossover peak between the  $F = 3 \rightarrow F' = 4$  and  $F = 3 \rightarrow F' = 3$  D2 lines. Before the split beam went into the spectroscopy alignment, its frequency was shifted down twice the modulating frequency by double passes the first acousto-optical modulator (AOM1) with a center frequency (CF) of 110 MHz from ISOMET (Part No.: 1206C). A homebuilt driver was used for modulating this AOM1.



During the experimental operation, it was necessary to shift the frequency of the cooling beam without changing the beam alignment. For doing that, the cooling beam was passed twice an AOM2 with a 75 MHz CF from Interaction (Part No.: ATM-751A2) as seen in Figure 4.4. An Interaction Model DE driver was employed for modulating the AOM2. After passing the AOM2, the beam was passed another Interaction AOM, or AOM3 used for fast switching the beam power. The first order of the cooling beam propagated through a mechanical shutter while the zero and other orders were blocked. All drivers received voltage signals from a computer control, for adjusting both the frequency and the intensity of the beams. Finally, the beam was sent through a half-wave plate and a PBS to align the direction of the linear polarization before it was coupled into a single mode fiber.

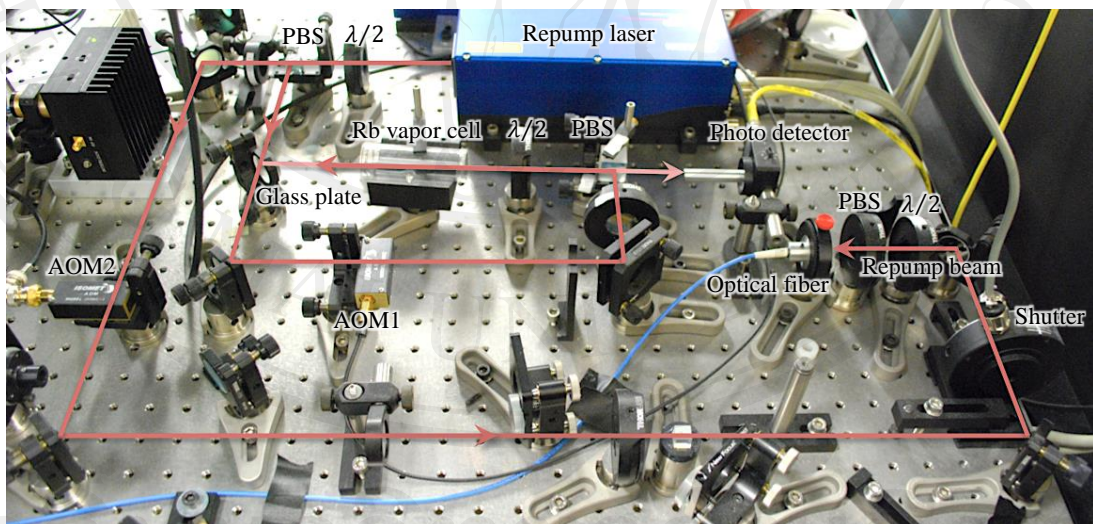


**Figure 4.5.** Photograph showing the optical alignment of locking and shifting the frequency for the repump laser.

For generating the MOT repump beam, a Toptica DL Pro ECDL was used as shown in Figure 4.5. The repump frequency was lock at a crossover peak between the  $F = 2 \rightarrow F' = 2$  and  $F = 2 \rightarrow F' = 3$  D2 lines by using PSAS. An AOM1 driven by a home-built modulator was put in the spectroscopy alignment. This gave us the shifted frequency of the repump beam that was equal to half of the modulating frequency of the AOM1. In this spectroscopy, only single photo detector was used that provided the absorption signal with the Doppler profile. The remaining repump beam was passed another AOM2 with 80 MHz CF from ISOMET (Part No.: 1205C-1) driven by another home-built modulator before propagated trough a mechanical shutter and was coupled in to a single mode fiber.

To calculate the cooling beam and the repump beam detunings from the  $F = 3 \rightarrow F' = 4$  D2 line transition and the  $F = 2 \rightarrow F' = 3$  D2 line transition respectively, the frequency shifting due to the locking point and the three AOMs was accounted that is:

$$\delta_{MOT} = \text{Lock frequency} (= -60.3 \text{ MHz}) - 2 \times \text{AOM1} + 2 \times \text{AOM2} + \text{AOM3},$$

$$\delta_{rep} = \text{Lock frequency} (= -31.5 \text{ MHz}) - \frac{1}{2} \times \text{AOM1} + \text{AOM2}.$$

After the MOT/cooling beam propagated through the optical fiber, the fiber steered the beam to where the science chamber was. The output beam from the other end of the fiber was split equally into three beams. The MOT beams were aligned quite similarly as for loading the MOT of the QAO Laboratory detailed in Chapter 3. The alignment of the MOT beams for passing through the view ports of the science chamber is shown in Figure 4.2. The repump beam output from the fiber was directly passed through one of the chamber windows. All beams were intersected at the center

of the chamber where a magnetic trap potential was minimum. The magnetic field was created by using a pair of magnetic coils mounted on two 2<sup>3</sup>/<sub>4</sub>-inch flanges. The coils consisted of 30 turns of copper wire with a radius of 6.5 cm. The current of 31 Amps was applied for providing the magnetic field gradient of 7.7 Gcm<sup>-1</sup> in the axial axis of the coils. The MOT was loaded for 50 ms by using the parameters of the light beams and the magnetic field gradient as detailed in Table 4.1 (the MOT powers mentioned are the measured power from only one of the MOT beams). Loading more atoms into the MOT with longer time (more than 2 second) does not lead to a significant increase in the number of atoms transferred to the FORT due to the tiny size of the FORT.

After the MOT stage, all of the parameters were ramped into the values used in a cMOT loading within duration of 1 ms. In the cMOT, the atoms were cooled by

**Table 4.1.** The cooling process with used parameters (the detuning and power of the beams and the magnetic field gradient) for loading Rb atoms into the FORT.

Process	Duration	MOT/cooling beam	Repump beam	Magnetic field gradient
MOT loading	50 ms	-14 MH, 4.5 mW	-5 MHz, 12 mW	7.7 Gcm <sup>-1</sup>
Ramp to cMOT	1 ms	↓	↓	↓
cMOT1	149 ms	-22 MH, 2 mW	-5 MHz, 2 mW	10.2 Gcm <sup>-1</sup>
cMOT2	1 ms	-22 MH, 2 mW	-5 MHz, 2 mW	↓
Ramp to Molasses	2 μs	↓	↓	Off
Molasses1	3 ms	-43 MH, 1 mW	-5 MHz, 2 mW	Off
Molasses2	2 ms	1 mW→Off	2 mW→Off	Off

using the further detuning of MOT beam and the lower repump power. At the same time, the atomic cloud was spatially compressed by the high magnetic field gradient. At the end of cMOT, the magnetic field gradient was ramped down until it was vanished. Finally, the MOT detuning was further adjusted and also reduced the power to load an optical molasses for 3 ms. All of the beams were then completely turned off in 2 ms at the end of the molasses loading. During this cooling and loading process, the dipole trap was left on all the time. As a result, the average of 10 to ~200  $^{85}\text{Rb}$  atoms were loaded into the trap depending on the MOT stage duration. The setup and calculation for the dipole trap is explained below.

#### 4.1.3 Optical dipole trap

To create the FORT, a far-red detuned light was focused by using the high NA lens mounted inside the science chamber. As mentioned before in Chapter 2, the atoms can be attracted into where the intensity of the red-detuned light is highest. In this experiment, a Sanyo laser diode (Part No.: DL8142-201) driven by a Thorlabs current and temperature controller (Part No.: ITC510) provided the dipole light beam at 828 nm wavelength. The beam propagated through an Interaction AOM (Part No.: ATM-1501A2) that acted as a fast switch for the beam. Amplitude of the AOM modulation was controlled by the voltage signal sending from the computer. The first order of the beam was passed through a pair of anamorphic prism for reducing an ellipticity of the beam before be coupled into an optical fiber.

After the dipole beam left the optical fiber, the beam emitted from the other end of the fiber was propagated through the high NA lens made from LightPath

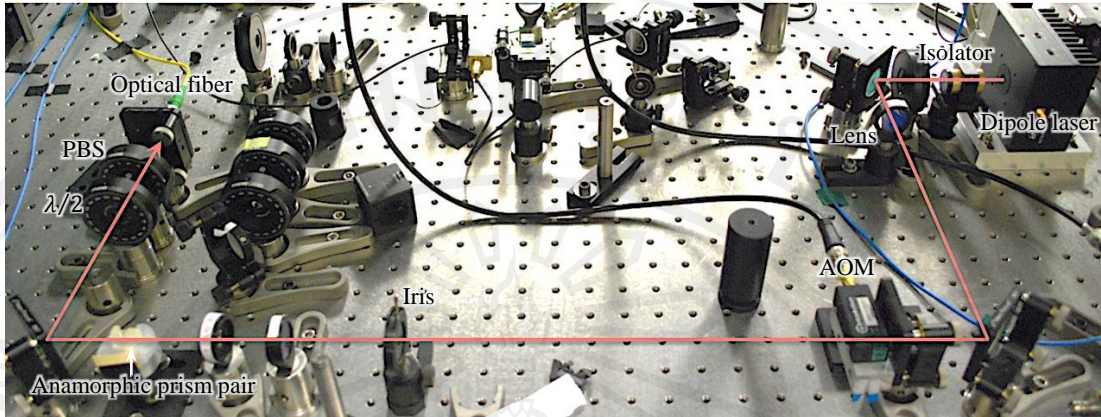


**Figure 4.6.** Photograph showing an optical alignment of switching AOM for a dipole laser.

Technologies (Part No.: 352230). As consequence, the dipole beam with the power of 30 mW was focused at the center of science chamber where the MOT cloud was formed. The beam waist,  $w_0$ , was measured by directly imaging the focus of the beam. The Gaussian fit to the measured waist gives us the value of  $1.8 \mu\text{m}$ .

The intensity distribution of the beam was calculated as a Gaussian beam, which is:

$$I(r, z) = \frac{2P}{\pi w^2(z)} \exp\left(-\frac{2r^2}{w(z)}\right), \quad (4.1)$$

where  $r$  is the radial distance from the center axis of the beam,  $z$  is the axial distance from the beam waist, and  $P$  is the power of the beam. Here the beam radius is given

by  $w(z) = w_0 \sqrt{1 + \left(\frac{z}{z_R}\right)^2}$ , where  $z_R = \pi w_0^2 / \lambda$  is called Rayleigh range. From the intensity distribution, the energy shift was calculated by using equation (2.13). Where

the Rabi frequency can be determined from  $\sqrt{\frac{3\lambda^3 \Gamma I}{4\pi^2 \hbar c}}$ , the energy shift is

$$\Delta E_i = \frac{3\pi c^2 \Gamma}{2\omega_0^3} I(r, z) \sum_j \frac{C_{ij}^2}{\delta_{ij}}. \quad (4.2)$$

The spatial dependent light shift of the energy level relative with the  $F = 2$  and  $F = 3$  ground states is represented in Figure 4.7. This shows a potential well with the depth of  $U_0 = h \times 85$  MHz corresponding with the trap depth of 4.1 mK.

In the FORT, the most trapped atoms took nearly all of the time around the bottom of the potential well or the center of the trap because the temperature of the atoms was very low (about  $300 \mu\text{K}$ ) compared with the trap depth. For this reason, the detuning of the lasers was included the maximum energy shift at the center of the dipole trap. The light-shifted-energy levels of the D1 and D2 lines are shown in Figure 4.8. The color arrows represent the relevant transitions used in the research.

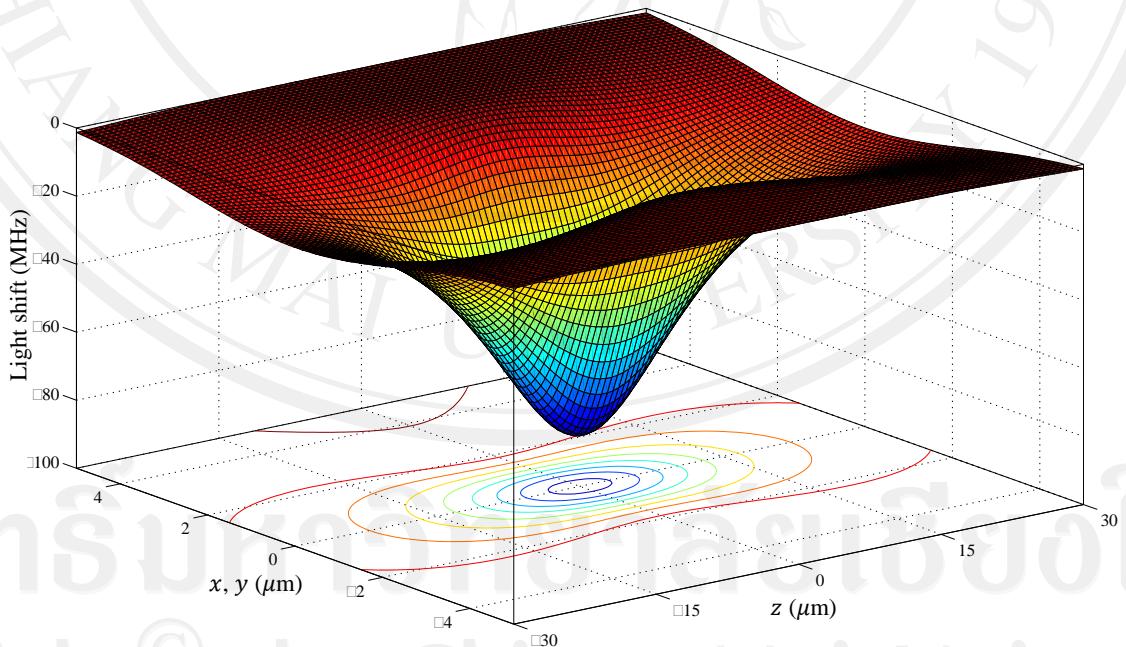


**Figure 4.7.** The energy shift of the atomic ground state plot as a function of the  $x, y$  and  $z$  positions where the origin is at the beam focal point.

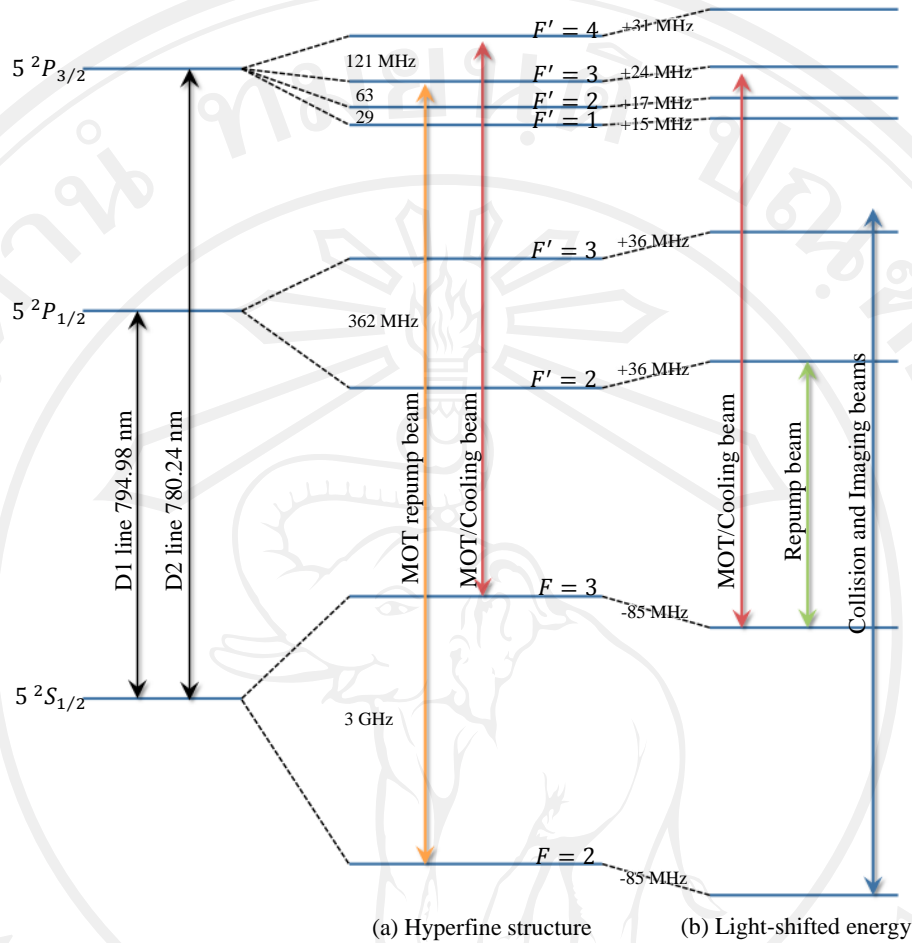


**Figure 4.8.** The energy level of  $^{85}\text{Rb}$  D lines transitions without the light (a) and the energy level shifted due to the presence of the light (b). Laser beams employed in this work with the corresponding transitions are shown.

#### 4.1.4 Imaging system and collision laser

For the fluorescence imaging, a standing wave of blue detuned light at 795 nm exposed the atoms trapped in the FORT. The light beam called imaging beam was linearly polarized and blue detuned by 15 MHz from the D1  $F=2$  to  $F'=3$  transition as seen in Figure 4.8. By using the imaging beam, the fluorescence of the

atoms in the  $F = 2$  ground state was induced and was corrected with the high NA lens. For the atoms in the  $F = 3$  ground state, they were optically pumped into the  $F = 2$  ground state by using a D1 repump beam which was red detuned by 20 MHz from the D1  $F = 3$  to  $F' = 2$  transition.

During imaging, the Doppler heating might be occurred because of the blue detuned imaging beam that lead to the loss of the atoms from the dipole trap. However, the standing wave of the imaging beam also produced the Sisyphus cooling mechanism (see section 2.1.5 in Chapter 2) to compensate with the heating. The Sisyphus cooling became dominant over the Doppler heating when the intensity of the imaging beam was high enough. Furthermore the six cooling beams used for loading MOT before were applied as well. These cooling beams provided the PGC mechanism (for more details in PGC see section 2.1.4) operating on the D2  $F = 3$  to  $F' = 4$  transition when the atoms were in the wings of the trap. At the bottom of the trap, the frequency of cooling beams closely corresponded with the D2  $F = 3$  to  $F' = 3$  transition (about  $-4$  MHz detuning). As a result, the cooling beams acted as the repump beam that optically pumped the atoms from the  $F = 3$  ground state to the  $F = 2$  ground state where they interacted with the imaging beam. Thus these beams are called “cooling/repumping beams” in this thesis.

Toptica DL Pro ECDL was used to provide a light with wavelength of 795 nm operating on the D1 transitions. Figure 4.9 shows a photo of the D1 laser and the optical alignment for controlling and stabilizing its frequency. The output beam was split a few mW into a PSAS for locking the laser frequency to the  $F = 2$  to  $F' = 3$  D1 transition. An Isomet AOM (Part No.: 1206C) labeled AOM1, was use to shifted

the laser frequency inside the PSAS by a half of the modulating frequency. The AOM1 was modulated by a home-built driver.

The remaining beam was split again by using a half-wave plate and a PBS2 into two beams. The first beam was the D1 repump beam was double passed through an AOM2 with a CF of 1.5 GHz from Brimrose (Part No.: GPF-1500-200-780) and was allowed only the first minus order to be reflected back to the PBS2. Agilent Signal Generator (Part No.: N5183A). This AOM2 was modulated by using a Mini-Circuits Power Amplifier (Part No.: ZHL-5W-2G). From this configuration, the frequency of the repump beam was shifted down by 3.15 GHz that corresponded to the  $F = 3$  to  $F' = 2$  D1 transition. For the second beam, it was passed through an AOM3 made from Interaction (Part No.: ATM2251A2). An Interaction Model DE driver was operated to modulate the AOM3. After the beam passed through the AOM3, the first order beam diffracted by this AOM was reflected back to the PBS2. This beam called a collision beam was used for inducing collisions between trapping. The zero-order beam diffracted from the AOM3 was used as an imaging beam. The imaging beam was double passed an Interaction AOM4 (Part No.: ATM1501A) modulated by an Interaction Model DE driver. Then the imaging beam propagated back to the PBS2 as well. As all of the three beams were combined at the PBS2, they have the same direction and were passed through an AOM5, which operated as a fast shutter. The AOM5 was an Interaction AOM (Part No.: ATM1351A) and was modulated by an Interaction Model DE. The first diffracted order from the AOM5 was coupled into a single mode fiber. The detuning of the three beams were calculated as:

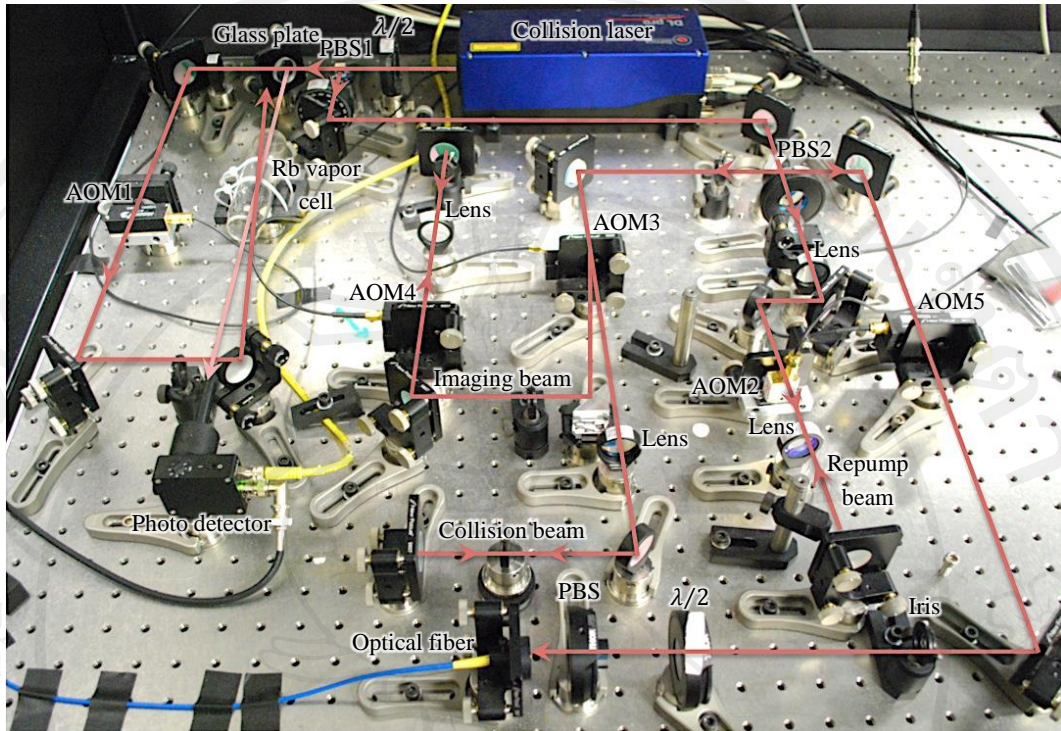


**Figure 4.9.** Photograph showing the optical alignment of locking and shifting the frequency for the D1 laser.

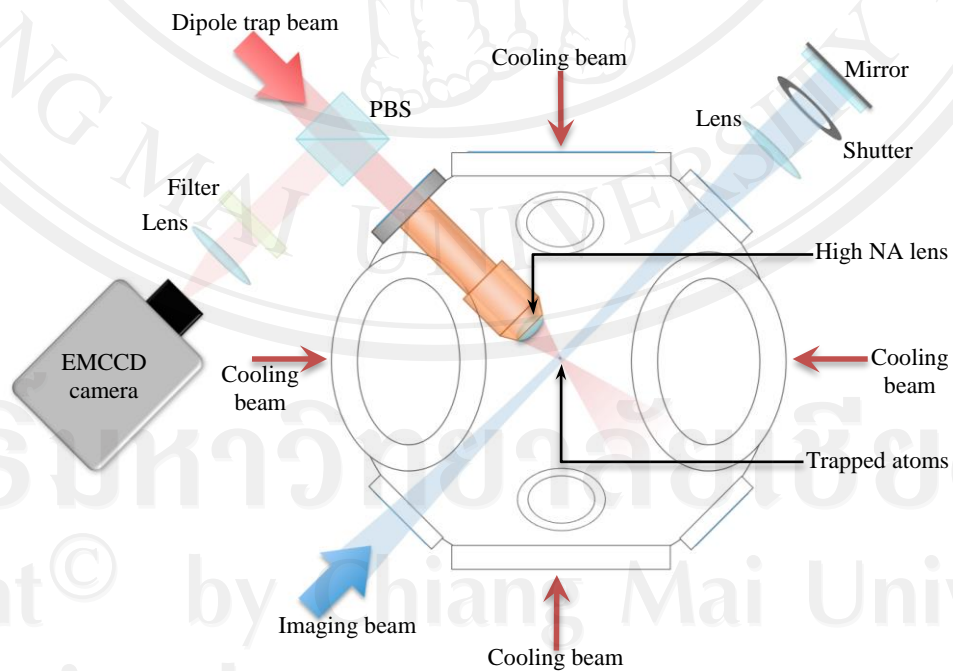


**Figure 4.10.** The schematic of the dipole trap and the imaging system.

$$\delta_{ima} = \text{Lock frequency (= 0 MHz)} + \frac{1}{2} \times \text{AOM1} + 2 \times \text{AOM4} - \text{AOM5},$$

$$\delta_{rep} = \text{Lock frequency (= +3.36 GHz)} + \frac{1}{2} \times \text{AOM1} + 2 \times \text{AOM2} - \text{AOM5},$$

$$\delta_{col} = \text{Lock frequency (= 0 MHz)} + \frac{1}{2} \times \text{AOM1} + 2 \times \text{AOM3} - \text{AOM5}.$$

After the three beams left from the fiber, they were steered into the science chamber by using many mirrors in such the way that their direction was overlapped the position of the dipole trap as illustrated in Figure 4.10. The beams were passed through a lens with the focal length of 500 mm before going into the chamber. After the beams left from the chamber, they were collimated by passing another lens and reflected off a mirror to go back into the science chamber for creating the standing wave. A mechanical shutter was installed in front of the mirror and turned the shutter on when the collision beam was employed. In the imaging stage, the imaging beam, the repump beam and the cooling/repumping beams with the power of  $40 \mu\text{W}$ ,  $15 \mu\text{W}$  and  $0.6 \text{ mW}$  respectively were applied. After the trapped atoms absorbed the photons and spontaneously emitted them, the high NA lens collected only about 10% of the fluorescence. The collected fluorescent light was passed a PBS. Approximately half of the light was reflected into another direction for separating them from the dipole beam as seen in the figure. The reflected light propagated through an 830 nm notch filter from Semrock (Part No.: NF0183OU) for removing the scattered light of the 828-nm dipole beam. Then the light propagated through a 795 nm bandpass filter (Part No.: FF01-800/12) for filtering other stray light. The output of the two filters, which was about 37% of the collected light, was focused onto an  $8.2 \times 8.2 \text{ mm}$  image sensor of an electron-multiplying charge coupled device (EMCCD) camera from Princeton Instruments (ProEM: 512B) to record the  $250 \times 30$  pixels images. A

measured quantum efficiency of the EMCCD was 60%. The EMCCD was cooled to  $-70\text{ }^{\circ}\text{C}$  by using a thermo-electric device for reducing a dark current. The avalanche e gain, which is an electron-multiplying gain of the EMCCD, was set at 100.

## 4.2 Trapped atoms detection

In this section, the techniques for preparing and counting a small number of atoms in FORT are explained (Section 4.2.1). These techniques were used to prepare and identify single and two atoms for the collisional study. The trapping lifetime and the temperature of the prepared single atoms were observed (Section 4.2.2). Finally, the method to determine an atom number for large samples in the trap was introduced (Section 4.2.3).

### 4.2.1 Preparation and counting small numbers of atoms

As the purpose of this thesis is to study the cold collisions between only two atoms, a method to prepare small numbers of atoms in FORT is needed. In this section, the preparation method using the light-assisted collision is introduced. The method is separated into three steps as illustrated in Figure 4.11. In the first step (Figure 4.11 (a)), by using the series of cooling and trapping techniques mentioned in Section 4.1.2, the average of 10 to 200  $^{85}\text{Rb}$  atoms were loaded into the dipole trap. The number of loaded atoms depended on both the loading times of MOT and cMOT. For the second step (Figure 4.11 (b)), the collision light pulse was applied for inducing the collisions between them where the light pulse consisted of the collision beam and the

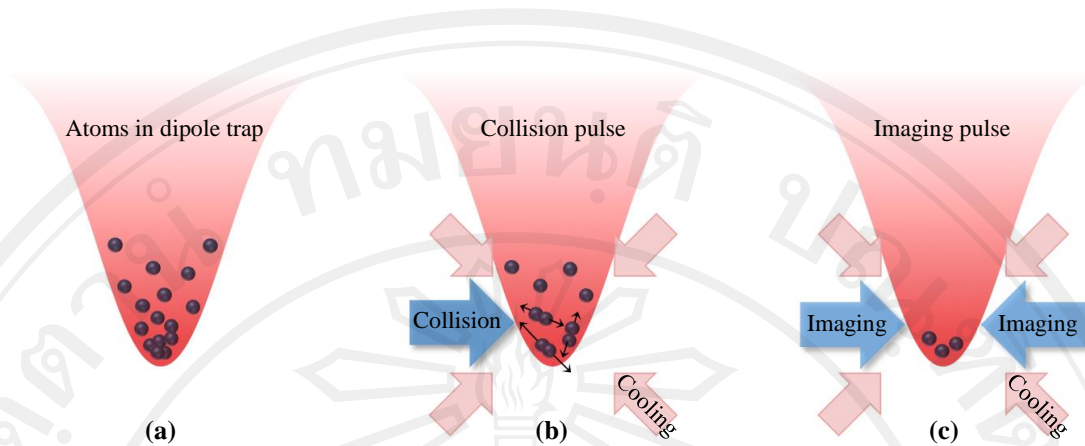


**Figure 4.11.** Preparation of small number of atoms by using the light-assisted collisions. The cold atoms are loaded into FORT (a); most of them are ejected out of the trap by the collision light pulse (b); and the remaining atoms are counted by using the imaging light pulse (c).

cooling/repumping beams (for more details, see Section 4.1.4). As a result, the majority of the atoms were ejected until only few atoms were left in the trap.

For the last step (Figure 4.11 (c)), the imaging stage was employed. The imaging light pulse exposes the remaining atoms for 10 ms. The light pulse consisted of the standing wave of the imaging beam, the D1-line repump beam and the cooling/repumping cooperating of the PGC and Sisyphus cooling provided the longer trapping lifetime of the atoms during the imaging stage. The fluorescence of the atoms induced by the imaging light was collected and focused into the EMCCD. The samples of the atomic fluorescence images are shown in Figure 4.12 (a). The images of the atoms were cropped into  $11 \times 11$  pixels frame.

The atomic fluorescence signals gained from the images were used to determine the numbers of atoms. An ADU number of each pixel in the image

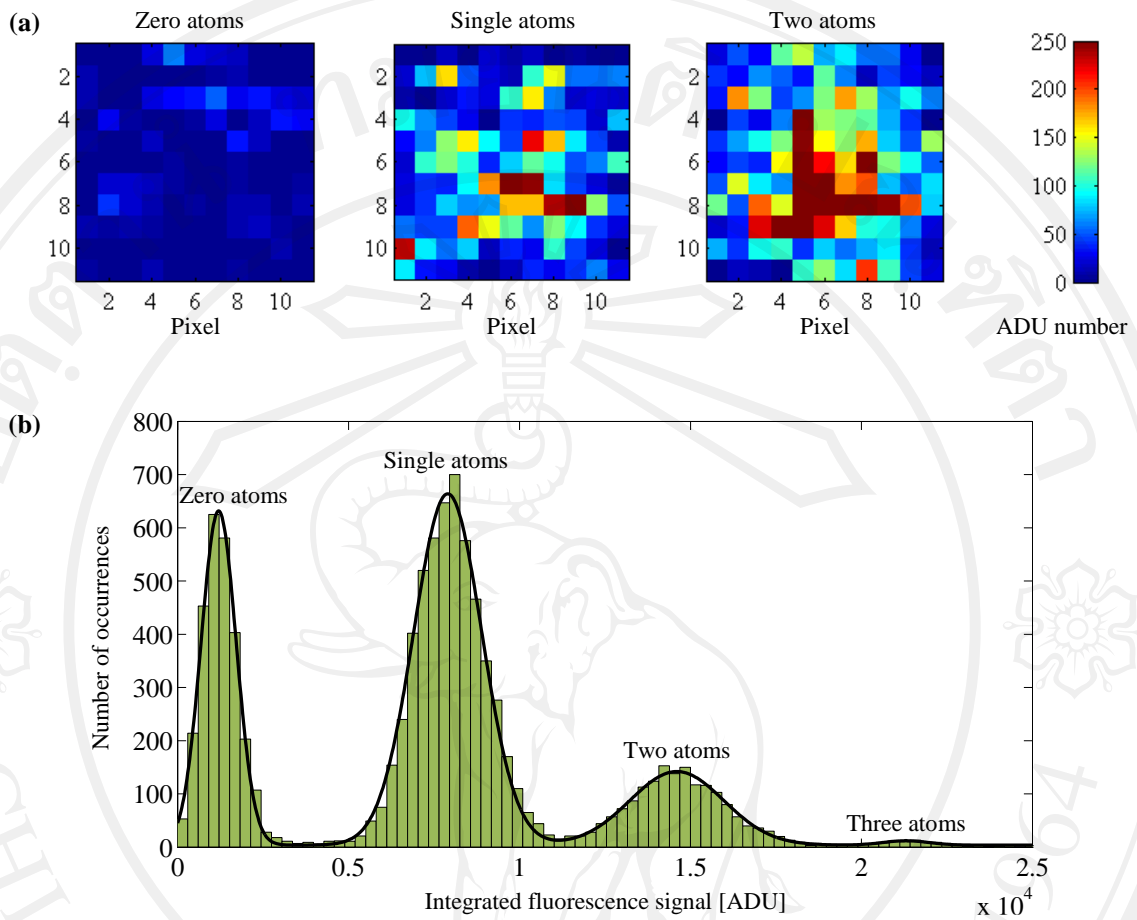


**Figure 4.12.** Experimental images of zero, one and two atoms are shown in (a). The color of each pixel is indicated an analog-to-digital unit (ADU) number of the atomic fluorescence as presented in the color bar. Histogram of the integrated fluorescence of each image for 10,000 experimental runs is plotted in (b). The peaks from the left hand represent zero, one, two and three atoms remaining in the FORT. The solid line indicates a fitting with the four Gaussians.

represented the level of the collected light intensity. Then a sum of the ADU numbers for the entire frame was done for getting an integrated fluorescence signal. For this method, only one experimental run cannot determine the atom number. Consequently, the all of these three steps was repeated several times (above 100 times in this

research). The histogram of the integrated fluorescence signals was plotted as shown in Figure 4.12 (b). The result shows that the appeared peaks are separated equally from the adjacent ones. That is because the atomic fluorescence was discrete in correspondence with the number of atoms in the trap. The peaks from the left hand represent the fluorescent signal from zero, one, two and three atoms remaining in the FORT respectively. The fluorescent signal for zero atoms is not equal to zero ADU due to the noise created from the EMCCD readout and the stray light. The photons emitting from the atoms follow a Poissonian photon statistic that contributes to the peak widths. However, by using this imaging technique, it is hard to resolve the peak of the high atom number due to the atomic lost during the imaging stage. The technique to determine the high number of atom will be presented later in Section 4.2.3.

In order to prepare either single or two atoms, the duration of the collision pulse in the second step was optimized. The imaging technique in the third step provided the capability to distinguish the number of atoms in each run. After the experiment was done for several runs, each run that either single or two atoms were loaded, was chosen to be accounted. In this work, the efficiencies of the preparations were about 0.40-0.90 for single atom and about 0.2-0.3 for the two atoms that depended on the parameters of the collision light pulse.

#### **4.2.2 Lifetime and temperature measurement**

After the single atoms and the pairs of atoms were prepared in the FORT, the trapping lifetime and the temperature of the atoms were measured. In this study, the lifetimes

of single atoms were measured under the influence of light. Figure 4.14 shows the measurement of the trapping lifetime of the single atoms while the collision pulse was being applied.

The lifetime measurement began with identifying the existence of single atoms by the imaging stage (which is the third step of preparing small number of atom in Figure 4.11 (c)). At this stage, the imaging pulse was applied for 10 ms as represented by the first blue pulse in Figure 4.13. Then the collision light pulse (the second pulse in the figure) was applied for the duration of  $\Delta t$ , where the pulse consisted of the collision beam with the power of 11 mW and the detuning of 85 MHz from  $F = 2$  to  $F' = 3$  D1 line transition and the cooling/repumping beams. During this duration, the atoms may be lost due to the radiative force of the light. Finally, the atom number left in the trap that could be either zero or one atom was measure by the second imaging stage. The experiment run was repeated for 200 times. Only the runs, which observed single atom in the first imaging state, were accounted. Then the probability of single atom remaining in the trap after applying the collision pulse is defined by

$$P_{Rem} = \frac{N(1)_2}{N(1)_1}, \quad (4.3)$$

where  $N(1)_i$  is the number of the experimental runs that found single atoms in the  $i^{th}$  imaging stage.

The remaining probability  $P_{Rem}$  getting from 200 experimental runs was plotted versus the pulse duration of  $\Delta t$  as shown in Figure 4.14. The blue circles indicate the observed  $P_{Rem}$  and the solid line is fitting curve calculated from the exponential decay function. The fitting function is:

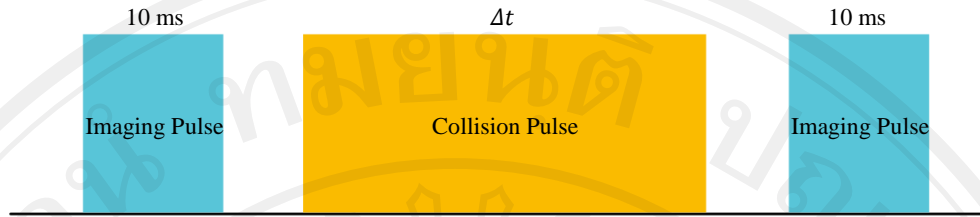


**Figure 4.13.** Schematic of the trapping-lifetime measurement.

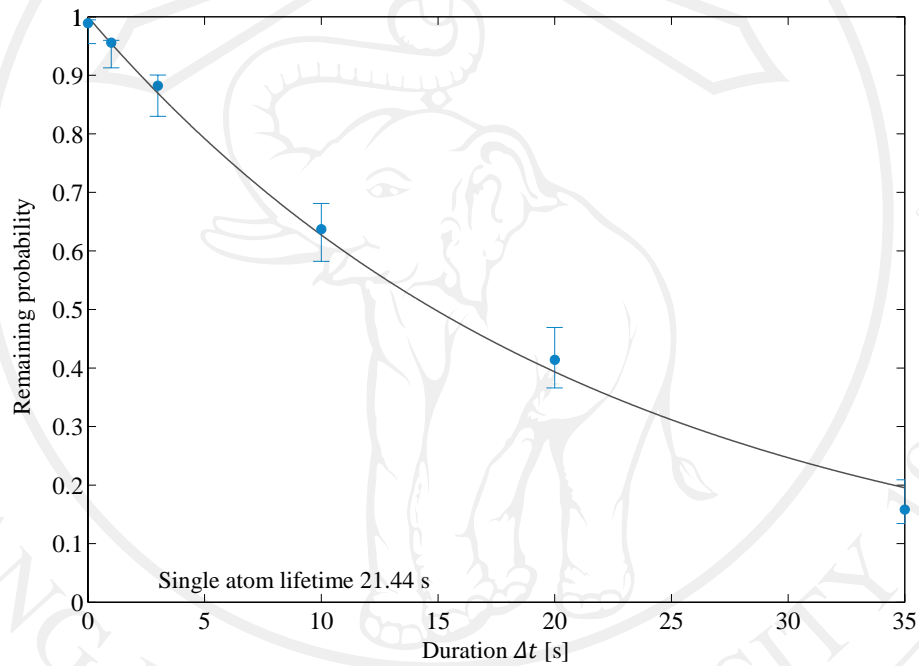


**Figure 4.14.** Remaining probability of single atom  $P_R$  plotted as a function of the duration  $\Delta t$ . The fitting provided the trapping lifetime of single atoms.

$$P_{Rem} = \exp\left(-\frac{\Delta t}{\tau}\right), \quad (4.4)$$

where  $\tau$  is the trapping lifetime of single atom. From the fitting, the trapping lifetime of single atoms under the influence of the blue detuned collision pulse is equal to 21.44 ms.

For the temperature measurement, a release and recapture method was used [50]. After the single atom was loaded into the FORT, the first imaging pulse was applied to identify the existence of single atom as represented by the first blue pulse in Figure 4.15. The FORT represented by the red pulse in the figure was turned off for the duration of  $\Delta t$ . With out the trapping beam, the atom was released to fly out off the trap with an initial velocity and also be force to drop down due to the gravity. At the end of the duration  $\Delta t$ , the trap was turned on again. The atom might be recaptured as the potential well was appeared. The number of atom in the FORT was measure at the end of process by the second imaging stage, which is represented by the second imaging pulse in the figure. As it was only one atom before tuning off the trap, the number measured by the second imaging could be either zero or one atom. The experimental run was repeated for 200 times. In the consequence, the probability that the single atoms were recaptured when the FORT was turned on is defined by

$$P_{Rec} = \frac{N(1)_2}{N(1)_1}, \quad (4.5)$$

To find out the temperature, the measured  $P_{Rec}$  was plotted versus the releasing duration of  $\Delta t$  as represented by the blue circle in Figure 4.16. The solid line represents the fitting data obtained from the Monte Carlo simulation. The fitting provided the estimated temperature of  $204 \pm 5 \mu\text{K}$ .

In the simulation, an  $^{85}\text{Rb}$  atom at trial temperature  $T$  was generated. The Maxwell-Boltzmann statistics was used for determining the initial velocity of the atom. Each one-dimensional velocity was chosen randomly from the normal distribution,

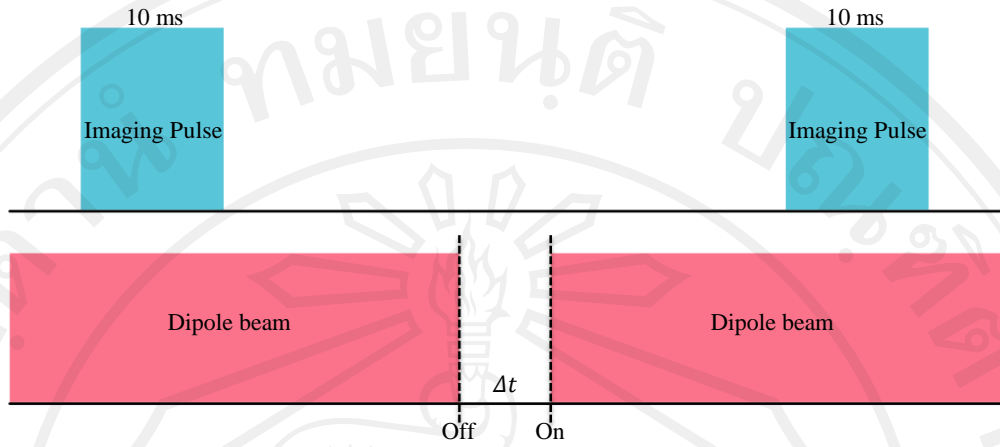


**Figure 4.15.** Schematic of temperature measurement by using the released and recaptured method.

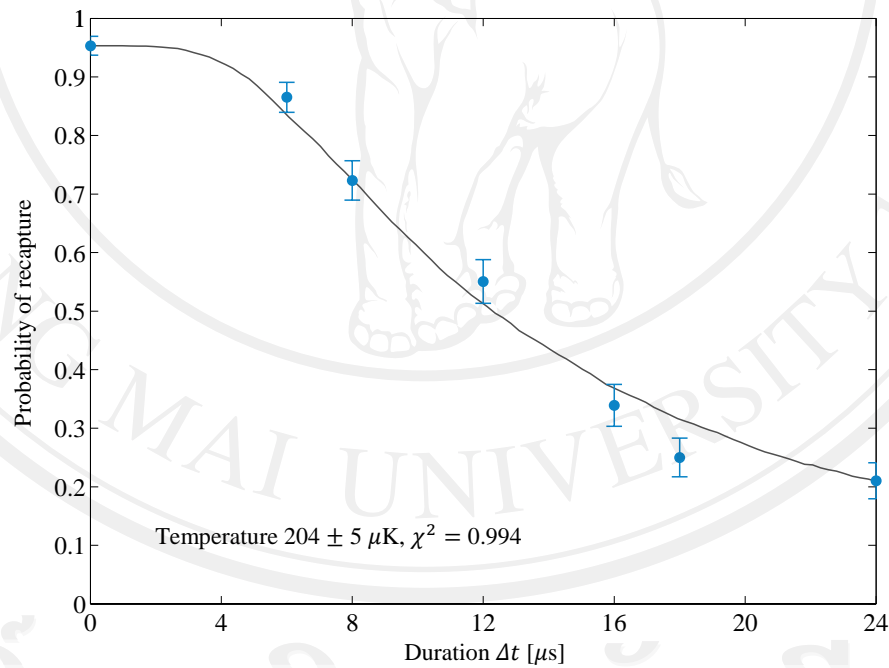


**Figure 4.16.** The Probability of recapture  $P_{Rec}$  is plotted against the releasing duration of  $\Delta t$ . The fitting line obtains from a Monte Carlo simulation explained in text to extract the temperature of  $204 \pm 5 \mu\text{K}$ .

$$f_v(v_i) = \frac{1}{\sigma\sqrt{2\pi}} \exp\left(-\frac{v_i^2}{2\sigma}\right), \quad (4.6)$$

where  $\sigma = \sqrt{\frac{k_B T}{m}}$ . The trapping potential was estimated as the harmonic one. That is

$$U(x, y, z) = -U_0 + \frac{1}{2}m[\omega_{rad}^2(x^2 + y^2) + \omega_{ax}^2 z^2], \quad (4.7)$$

where  $U_0$  is a depth of the dipole trap,  $\omega_{rad}$  and  $\omega_{ax}$  are the natural oscillation of the atom in the harmonic trap in the radial and axial directions respectively. The initial position of the atom in the radial and axial directions were chosen randomly from the normal distribution where  $\sigma_{rad} = \sqrt{\frac{k_B T}{m\omega_{rad}^2}}$  and  $\sigma_{ax} = \sqrt{\frac{k_B T}{m\omega_{ax}^2}}$  respectively. The starting time of the simulation was set as the time when the trap was turned off. Then the position and velocity of the atom evolved dynamically in time under the influence of the gravity force. Each time steps of simulation, the possibility that the atom was recaptured when the trap was suddenly turned on, was observed. The atom was considered to be lost if its kinetic energy of was higher than the depth of the trapping potential at that position. The simulation was continued until the time was equal to the longest experimental duration. These processes were repeated for 5,000 single atoms to get the average value of  $P_{Rec}$  as a function of the duration. The temperature  $T$  was varied until the simulating  $P_{Rec}$  curve fit well with the experimental data. The programming of the simulation is shown in Appendix B.

The temperature of the atomic pairs in the trap was also measured by using the same method. Figure 4.17 shows the experimental result and the fitting solid line that determine the temperature of  $281 \pm 14 \mu\text{K}$ . The temperatures of the single atoms and

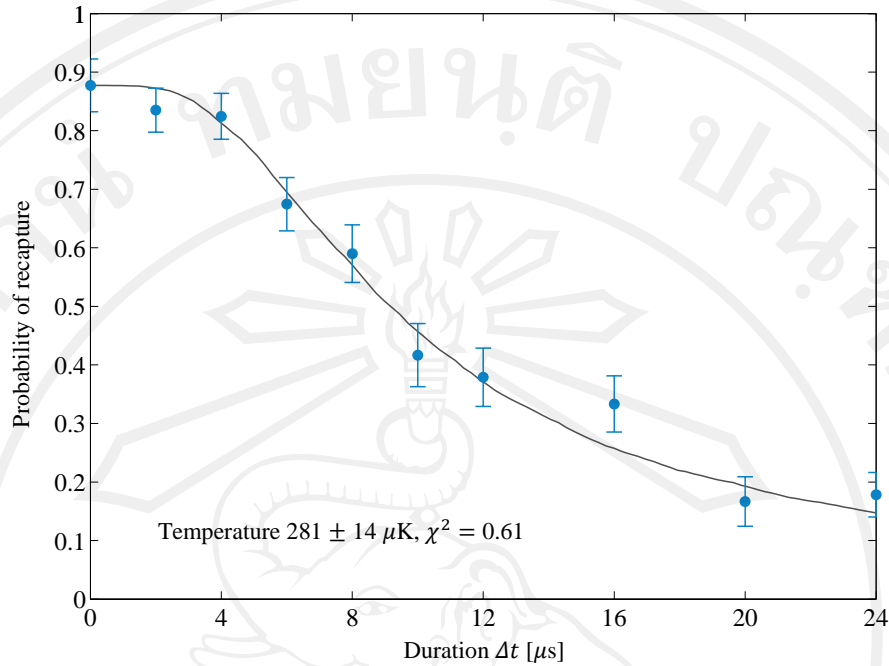


**Figure 4.17.** The result of temperature measurement for the atomic pair in the dipole trap. The Probability of recapture is plotted against the release duration. The fitting line obtained from a Monte Carlo simulation extract the temperature of  $281 \pm 14 \mu\text{K}$  from the release and recapture data.

the pairs were used for determining in the study of the cold collision, which is detailed in the next chapter.

### 4.2.3 Determining the atom number in the trap

To determine the number of atoms in the trap, it was necessary to account the effect of atomic collisions induced while the imaging pulse exposed the atoms. The losing rate of the atoms due to the collisions increased relatively with the atomic number in the trap as represented in equation (2.16) in Chapter 2. During imaging state, the changing rate of the atom number in the dipole trap can be calculated by

$$\frac{dN}{dt} = -\gamma N - \beta N(N - 1). \quad (4.8)$$

Here the atomic loading rate of the dipole trap is zero and the rate of atomic loss due to the light induced two-body collisions is proportional to  $N(N - 1)$ , where  $N$  is the number of atom [51]. Equation (4.8) is transformed into  $dN \left( \frac{1}{N} + \frac{1}{\alpha - N} \right) = A dt$ , where  $A = \beta - \gamma$  and  $\alpha = A/\beta$ . Integrating both side of the equation gives us the result of

$$N = \frac{\alpha}{\frac{1}{B} e^{-At} + 1}, \quad (4.9)$$

where  $B$  is a constant getting from the integration. In case of  $t = 0$ , the number of atom is equal to  $N_0$ . Substituting this in Equation (4.9) gives us  $B = \frac{N_0}{\alpha - N_0}$  and the equation is changed into:

$$N(t) = \left[ \frac{\beta}{A} + \left( \frac{1}{N_0} - \frac{\beta}{A} \right) e^{-At} \right]^{-1}. \quad (4.10)$$

For determining the number of atoms in the trap, the total fluorescence signal of the trapped atoms was observed as a function of the exposure time of imaging pulse  $\Delta t$ .

The total fluorescence can be calculated by  $\int_0^{\Delta t} F_1 N(t) dt$ , where  $F_1$  is the average of measured fluorescent rate of single atoms. As a consequence, the total fluorescence is determined by

$$F_{tot}(\Delta t) = F_1 \left[ \frac{A\Delta t}{\beta} + \frac{1}{\beta} \ln \left( \frac{\beta N_0}{A} + \left( 1 - \frac{\beta N_0}{A} \right) e^{-A\Delta t} \right) \right]. \quad (4.11)$$

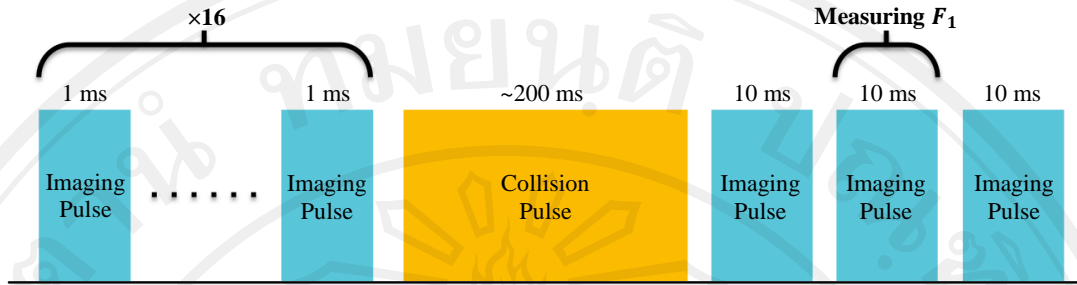


**Figure 4.18.** Schematic of the atom-number measurement.

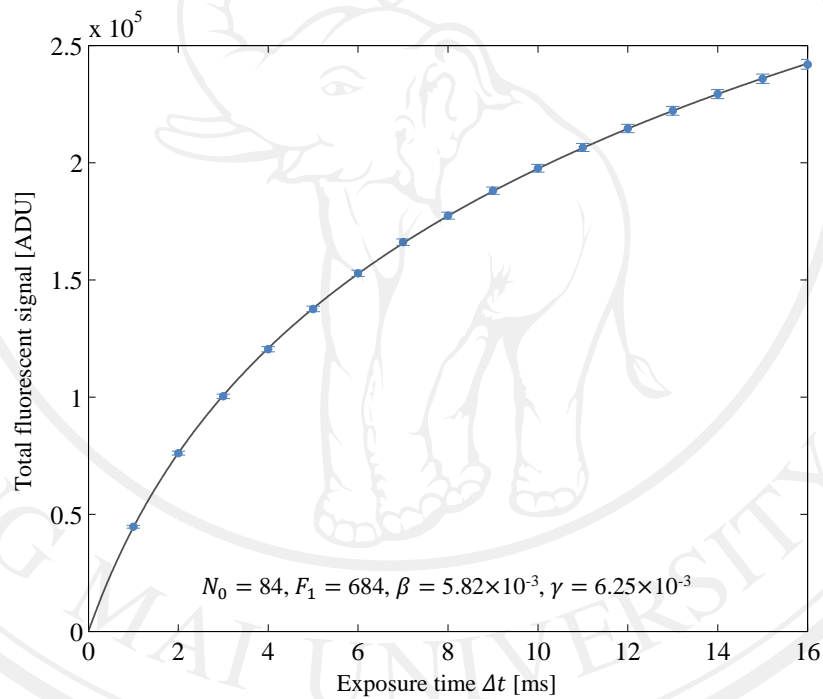


**Figure 4.19.** Total fluorescent signal of the remaining  $^{85}\text{Rb}$  atoms in the dipole trap versus the exposure time of imaging pulse.

In the experiment, after cold atoms were loaded into the FORT, the series of fluorescence images were recorded as shown by the 16 imaging pulses in Figure 4.18.

For each image, the detector collected the atomic fluorescence for a duration of 1 ms.

Then the collision light pulse was used to eject the atoms out off the trap until only

single atom left. To measure  $F_1$ , three imaging stages with the duration of 10 ms were applied as shown in the figure. The experiment was repeated for 200 runs to obtain the average value. Only the fluorescence signals obtained from the second imaging stages of the experimental runs that single atoms were found in both the first and last imaging states, were counted for determining  $F_1$ .

The fluorescence signals obtained from the 1-ms imaging pulse were accumulated for getting the total fluorescence signal as a function of the exposure time of the imaging pulse as plotted in Figure 4.19. The result was fitted with Equation (4.11) as represented by the solid line. This fitting provided the initial number of atoms  $N_0$  before shining the imaging light pulse. As the result, the initial number of atoms was equal to 84 and during apply the light pulse they were lost from the trap with the rates  $\gamma = 6.25 \times 10^{-3} \text{ s}^{-1}$  and  $\beta = 5.82 \times 10^{-3} \text{ s}^{-1}$ .